Monolayer Formation of a Pt–Ru Dinuclear Complex on a Gold (111) Surface and Its Conversion to a Pt–Ru Two-dimensional Nanocomposite Having Electrocatalytic Activity

Hiromitsu Uehara,[1] Yukihisa Okawa,[1] Yoichi Sasaki,[1] and Kohei Uosaki[*1,2]
[1]*Division of Chemistry, Graduate School of Science, Hokkaido University, Kita-ku, Sapporo 060-0810*
[2]*International Center for Materials Nanoarchitectonics Satellite (MANA), National Institute for Materials Science (NIMS), Kita-ku, Sapporo 060-0810*

Monolayers of Pt–Ru hetero-dinuclear complex were prepared on a Au(111) surface to obtain a designed two-dimensional Pt–Ru nanocomposite that acts as electrocatalyst for methanol oxidation reaction in alkaline solution.

Direct methanol fuel cell systems (DMFCs) are promising power sources for portable devices, since they use a liquid material, methanol, as a fuel. In current DMFCs, platinum-based electrocatalysts are used for methanol oxidation reaction (MOR) and the formation of poisoning CO ad-layer (CO_{ad}) on the Pt surface is the most serious problem. To construct practical DMFCs, it is essential to remove the CO_{ad} species at relatively negative potential so that MOR proceeds at low overpotential. It is known that CO_{ad} species can be oxidized to CO_2 by adsorbed OH species, which are formed from partial oxidation of water.[1] Binary catalysts, specifically highly dispersed platinum nanoparticles with ruthenium species such as Ru^0, RuO_x, and/or RuO_xH_y, are considered to be a good electrocatalyst for MOR, because adsorbed OH species formed at the ruthenium site can oxidize CO_{ad} at relatively negative potential.[1,2] Thus the best synergetic effect for MOR catalyst is expected if the catalyst is atomically well-dispersed 1:1 Pt–Ru composite. To date, Pt–Ru materials generally used for MOR experiments have been prepared from platinum chloride and ruthenium chloride by chemical reduction or electrodeposition,[2a] and often suffer from phase separation.

Here we propose a novel method to construct well-dispersed Pt–Ru nanocomposite structure. First, a monolayer of a well-designed Pt–Ru hetero-dinuclear complex is formed on a solid surface and then the organic ligands are removed by heating. Pt and Ru atoms on the surface are in a fixed ratio of 1:1 as synthetically designed and closely placed within 1 nm as atomically-mixed $Pt_{50}Ru_{50}$ nanocomposite.

A new Pt–Ru complex, $[Pt^{II}(trpy)Ru^{II}(bpy)(trpy)(\mu\text{-}otdst)](PF_6)_2$ (trpy = 2,2′;6′,2″-terpyridine, bpy = 2,2′-bipyridine, H_2otdst = 2-octylthio-4,6-disulfanyl-1,3,4-triazine) (Figure 1, **1**) was designed for this purpose.[3] The precursor complex, $[Ru^{II}(bpy)(trpy)(Hotdst)](PF_6)$, and $[\{Pt^{II}(trpy)\}_2(\mu\text{-}dst)](PF_6)_2$ (H_2dst = 2,5-disulfanyl-1,3,4-thiadiazole) (Figure 1, **2** and **3**, respectively) were also used for comparative experiments.[4] The bridging ligand $otdst^{2-}$ with a long alkyl-chain was chosen to place the complex on a Au(111) surface in an ordered way. Successful construction of Pt–Ru nanocomposite of metallic Pt and Ru materials on a Au(111) surface with electrocatalytic activity for MOR by thermal decomposition of the monolayer was confirmed.

The complex **1** was deposited on a Au(111) substrate by immersing the substrate into acetone solution containing 100 μM **1**
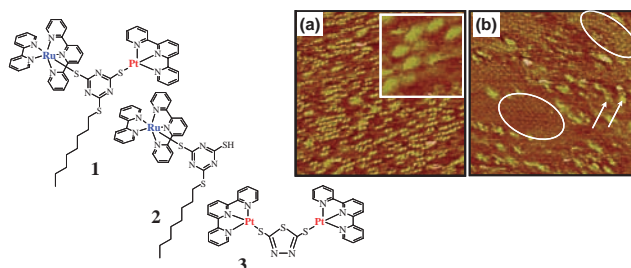

Figure 1. Schematic structures of Pt–Ru hetero-complex **1**, Ru complex **2**, and Pt complex **3** (left half). The right half is (a) an STM image ($40 \times 40\,nm^2$) of $\mathbf{1}_{ad}$/Au; (inset) high-resolution STM image ($5 \times 5\,nm^2$) $E_{bias} = 0.6\,V$, $I_{tc} = 0.1\,nA$. (b) An STM image of $\mathbf{1}_{heat}$/Au. $E_{bias} = 0.3\,V$, $I_{tc} = 0.5\,nA$. Typical Pt–Ru nanocomposits and elemental sulfur monolayer regions were indicated arrows and circles, respectively.

for 30 min ($\mathbf{1}_{ad}$/Au). The electrode thus obtained was then heated at 300 °C for 1 h to decompose organic ligands ($\mathbf{1}_{heat}$/Au).

Preadsorbed $\mathbf{1}_{ad}$/Au was characterized by means of scanning tunneling microscopy (STM). The STM image shown in Figure 1a reveals adsorbed molecular array structure. The molecules formed small domains without long-range order. From high-resolution STM image (Figure 1a, inset), the metal center area of each molecule was identified as a spot 1.2 nm in diameter and 0.25 nm in height. If we reasonably assume that the bridging ligand of **1** was laid on the surface parallel to the π plane of triazine ligand, the surface coverage of **1** estimated from typical STM images was approximately $5 \times 10^{-11}\,mol\,cm^{-2}$.

Surface morphology of the substrate after the heat treatment $\mathbf{1}_{heat}$/Au was also investigated by STM as shown in Figure 1b. Several grains (3 nm in diameter, arrows in Figure 1b) were dispersed on the electrode surface. In addition, as shown by the encircled area of Figure 1b, a terrace of Au(111) surface was covered with monoatomic layer domains of elemental sulfur that are close to $(\sqrt{3} \times \sqrt{3})R30°$ structure.[5] The sulfur atoms must have originated from pyrolyzed organic ligands. The STM images also indicate that the height of the grains was only 0.3 nm, indicating that nanocomposites grew only in two-dimensions, not in the vertical direction to form core–shell structure. Accordingly, it is possible that all the Pt and Ru atoms should be exposed to the interface.

Next we focus on electrochemical properties of $\mathbf{1}_{heat}$/Au in 0.1 M $HClO_4$. Figure 2a depicts CVs with multiple oxidation–reduction cycles (ORC) from -0.2 to 1.45 V vs. Ag/AgCl. While peak intensity of broad oxidation waves around 1.3 V decreased as potential cycles were repeated, the coupled sharp reduction wave at 0.93 V was unchanged. These results clearly show that the oxidation waves were composed of two components, one
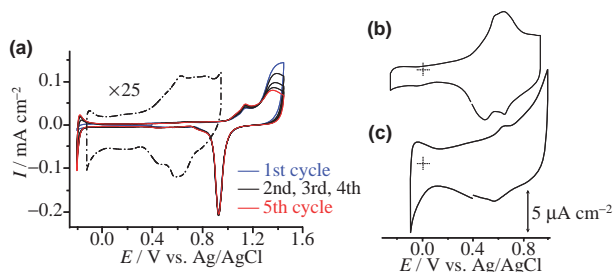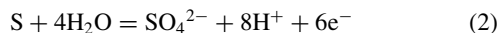
Figure 2. (a) Sequential change in cyclic voltammograms (CVs) of $\mathbf{1}_{heat}/Au$ while continuous potential cycles from -0.2 to $1.45\,V$ in $0.1\,M$ $HClO_4$. Scan rate $= 0.05\,V\,s^{-1}$. (blue) 1st cycle, (black) 2nd to 4th cycles, (red) 5th cycle. Dashed line shows enlarged double layer region of $\mathbf{1}_{ORC}/Au$. (b) and (c) CVs of double layer region of $\mathbf{2}_{ORC}/Au$ and $\mathbf{3}_{ORC}/Au$, respectively.

of which was not accompanied by the reduction. Thus, we assigned the overlapped anodic current due to the reversible oxidation of Au to AuO (eq 1) and irreversible oxidation of adsorbed sulfur atoms to water soluble sulfate ion (eq 2)[5]

$$Au + H_2O = AuO + 2H^+ + 2e^- \qquad (1)$$

$$S + 4H_2O = SO_4{}^{2-} + 8H^+ + 6e^- \qquad (2)$$

Cathodic current due to hydrogen evolution reaction (HER) at $-0.1\,V$ increased as potential scan was repeated. This is because oxidative removal of surface contaminated sulfur resulted in the increase of HER active-surface area (the HER-active electrode thus treated is defined as $\mathbf{1}_{ORC}/Au.$). It is noted that hydrogen adsorption/desorption current on platinum electrode, normally appeared between 0.1 to $-0.2\,V$ vs. Ag/AgCl region,[6] was not observed in this system as shown by a dashed line in Figure 2a with enlarged current scale, although the electrode had high HER activity. It has been reported previously that, if platinum is very highly dispersed, adsorption/desorption waves may not be observed.[7] The enlarged CV of $\mathbf{1}_{ORC}/Au$ (dotted line), however, showed anodic peak at $0.63\,V$ and cathodic peaks at 0.61 and $0.48\,V$. To clarify the origin of peaks, electrochemical behaviors of Au electrodes modified with single component, $\mathbf{2}_{ORC}/Au$ and $\mathbf{3}_{ORC}/Au$ (Figures 2b and 2c), which were prepared from $\mathbf{2}_{ad}/Au$ and $\mathbf{3}_{ad}/Au$, respectively, in the same manner as $\mathbf{1}_{ORC}/Au$, were investigated. Both $\mathbf{2}_{ORC}/Au$ and $\mathbf{3}_{ORC}/Au$ showed broad oxidation/reduction waves in the same area observed for $\mathbf{1}_{ORC}/Au$. The waves of $\mathbf{2}_{ORC}/Au$ and $\mathbf{3}_{ORC}/Au$ are assignable to the oxidation of Ru and Pt metals associated with OH adsorption/desorption, respectively.[8] The CV of $\mathbf{1}_{ORC}/Au$ is, however, not a simple superposition of those of $\mathbf{2}_{ORC}/Au$ and $\mathbf{3}_{ORC}/Au$, suggesting the interaction of the two metal centers. X-ray photoelectron spectra showed that the Pt:Ru ratio of $\mathbf{1}_{ORC}/Au$ was almost 1:1 as that of $\mathbf{1}_{ad}/Au$. These results suggest that well-mixed Pt–Ru nanocomposites were formed after the ORC treatment.

Finally, electrocatalytic activity of the Pt–Ru nanocomposite for MOR was briefly studied. Figure 3 shows CVs of (a) $\mathbf{1}_{ORC}/Au$ and (b) Pt (poly) foil in a $0.1\,M$ KOH solution containing $1\,M$ CH_3OH. Anodic peaks were observed in forward and backward scans in both cases,[9] showing that the 2D-nanocomposite surfaces were also MOR active. The smaller current at the 2D-nanocomposite modified surface should be due to the smaller number of Pt–Ru atoms and can be improved by increasing the number of repetitions of the modification process. More detailed
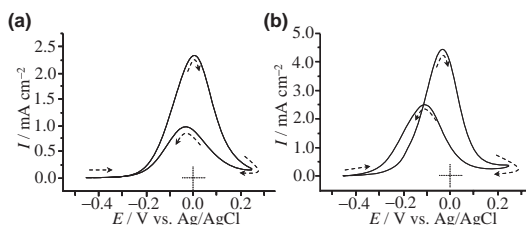

Figure 3. CVs for MOR in $0.1\,M$ KOH–$1\,M$ methanol solution. Scan rate $= 0.05\,V\,s^{-1}$. Electrode is (a) $\mathbf{1}_{ORC}/Au$, and (b) Pt(poly) foil.

analysis of the electrochemical response such as smaller peak separation is underway.

In conclusion, we have successfully formed a monolayer of new platinum(II)–ruthenium(II) hetero-binuclear complex onto a Au(111) electrode surface, and converted it into Pt–Ru nanocomposite. From STM images, the Pt–Ru nanocomposites are well dispersed on gold substrate in two dimensions. After the ORC treatment between -0.2 to $1.45\,V$ vs. Ag/AgCl, contaminated surface sulfur was removed and significant enhancement of electrocatalytic activities for HER and MOR were observed. The designed mixed-metal 2D-nanostructures on solid surfaces as patterned by the parent mixed metal coordination compounds is a promising approach to the fabrication of novel nanocomposite structures with electrocatalytic activity. The further study of the catalytic activity as well as the estimation of the local structure of active mixed platinum surface area is in progress.

References and Notes
1   A. Hamnett, *Catal. Today* **1997**, *38*, 445.
2   a) O. A. Petrii, *J. Solid State Electrochem.* **2008**, *12*, 609. b) C. Bock, M.-A. Blakely, B. MacDougall, *Electrochim. Acta* **2005**, *50*, 2401. c) D. R. Rolison, P. L. Hagans, K. E. Swider, J. W. Long, *Langmuir* **1999**, *15*, 774.
3   The complex **1** was synthesized from the reaction of **2** and $[Pt^{II}(trpy)(OH)](PF_6)$. Calcd for $\mathbf{1}\cdot H_2O$: C, 40.45; H, 3.26; N, 10.17; S, 6.35%. Found: C, 40.54; H, 3.13; N, 10.13; S, 6.42%. ESIMS: m/z 1351.1 ($[\mathbf{1} - (PF_6)]^+$).
4   Details of the complex **3** will be reported separately (H. Uehara, et al.).
5   a) C. Vericat, G. Andreasen, M. E. Vela, R. C. Salvarezza, *J. Phys. Chem. B* **2000**, *104*, 302. b) M. D. Lay, K. Varazo, J. L. Stickney, *Langmuir* **2003**, *19*, 8416.
6   D. Qu, K. Uosaki, *J. Phys. Chem. B* **2006**, *110*, 17570.
7   a) Y. Takasu, Y. Fujii, E. Enami, Y. Matsuda, *Chem. Lett.* **1986**, 445. b) J. Kim, C. Jung, C. K. Rhee, T. Lim, *Langmuir* **2007**, *23*, 10831. c) H. Hoster, B. Richter, R. J. Behm, *J. Phys. Chem. B* **2004**, *108*, 14780.
8   a) V. Climent, R. Gomez, J. M. Ort, J. M. Feliu, *J. Phys. Chem. B* **2006**, *110*, 11344. b) D. Galizzioli, F. Tantardine, S. Trasatti, *J. Appl. Electrochem.* **1974**, *4*, 57.
9   We note that the current density of Figure 3a is normalized by Au(111) electrode surface area because of lack of information of active platinum surface area for MOR from electrochemical estimation such as hydrogen adsorption.